Surface Cleaning Force Control of Rotating Brushes for an Air Duct Cleaning Robot

Wootae Jeong[1], Seung-Woo Jeon[2], Duckshin Park[1] and Soon-Bark Kwon[1]
[1]Eco-Transport Research Division, Korea Railroad Research Institute,Gyeonggi-do,Uiwang, Korea
[2]Department of Virtual Engineering, University of Science and Technology, Daejeon, Korea

Keywords: Force Control, Compliance Device, Kinematic Analysis, Service Robot, Air Duct Cleaning.

Abstract: Due to the complexity of the air duct and ventilation system, removing accumulated dusts and particular matters at inner surface of air duct system becomes key issue for improving indoor air quality and maintaining the green environment of underground facilities. Although various tools and technologies for air duct cleaning have been developed, mechanical brushing method is evaluated as the most effective method in cleaning duct and ventilation system. Therefore, automotive duct cleaning robot with rolling brushes has been developed in this study. In particular, by adding compliant force feedback sensors to the rolling brushes, the developed cleaning robot can control the cleaning force consistantly between brush and duct surface. Force feedback control algorithm has been also developed and evaluated through control simulation tools.

1 INTRODUCTION

The HVAC(Heating, Ventilating, and Air Conditioning) system that supplies fresh and clean air from outdoor environment has been utilized in most of closed spaces such as modern buildings and subway facilities where people work and spend most of their daily hours. Due to the complexity of the air duct and ventilation system and long period of cleaning and maintenance, various types of infiltrated particles and dusts are accumulated at inner surface of the duct without being exhausted. Figure 1 shows pictures of before and after cleaning duct. In general, the accumulated dusts and particles flow into the living space and influence on the human respiratory system and health. In addition, the accumulated dusts and particles can reduce the efficiency of the air conditioning and heating of the HVAC system reported by Brosseau et al., 2000 Furthermore, the closed structure of ducts provides a good propagating circumstance of microorganisms including viruses and bacteria. Recently some contraries have established the regulation and guideline for ventilation system cleaning (FiSIAQ, 2001), however, many countries still do not have legal regulations about cleaning ventilation systems.

Recently, the research and development of duct cleaning technology has been conducted widely as concerns and requests of improving air quality are increasing. In fact, duct cleaning techniques can be classified as a dry method such as blowing out with compressed air and scraping out using mechanical brush and a wet method spraying water or chemical solution. Especially, the mechanical brushing is widely used because of its higher cleaning efficiency and accessibility. Various types of robots with mechanical cleaning tools have been developed and used for specific air duct cleaning. However, many manual cleaning methods are still broadly being used in cleaning the HVAC systems.

Figure 1: Before cleaning Air duct and After Cleaning.

Therefore, in order to provide more efficient and autonomous mobile cleaning robot platform, a new mobile robot equipped with mechanical rotating brushes and sensors has been developed as shown in Figure 2. In particular, the duct cleaning robot can clean four sides of inner duct surface simultaneously

Jeong W., Jeon S., Park D. and Kwon S..
Surface Cleaning Force Control of Rotating Brushes for an Air Duct Cleaning Robot .
DOI: 10.5220/0004591104530457
In *Proceedings of the 10th International Conference on Informatics in Control, Automation and Robotics* (ICINCO-2013), pages 453-457
ISBN: 978-989-8565-71-6

and utilize spring-based force feedback compliant device to be adapted at irregular cleaning target surfaces of ducts.

In this paper, a force feedback control method is suggested to keep the constant cleaning brush pressure on the irregular duct surface with simple spring-based compliant devices. In addition, various simulations have been conducted to evaluate performance of the control method.

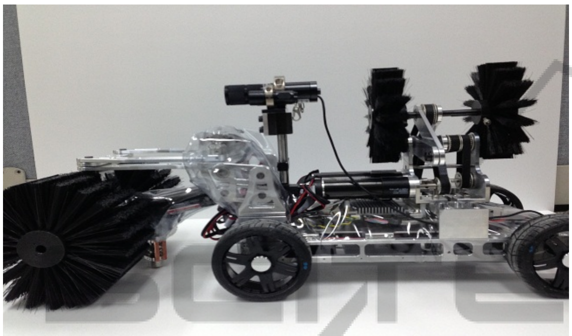

Figure 2: Prototype of Duct Cleaning Robot.

2 FORCE CONTROL USING COMPLIANT DEVICE

The pressing force of the rotating brush acting on the surface of the duct should be sustained constantly to remove the dusts accumulated firmly on the duct surface through many years. Higher cleaning pressure can damage duct surfaces and lower cleaning pressure may not be enough to remove the firmly attached dust and contaminants on the duct surfaces. Therefore, it is important to control the pressing force of the rotating brush constantly with respect to irregular surface of inner duct. This section describes modelling and control of the rotating brush with a spring-based force compliant device.

2.1 Modelling of the Mechanical Brush

The compliance device is composed of the linear spring, linear encoder and ball roller attached at the end of the spring not to resist for moving with rotating brush of the robot platform. Figure 3 shows the free body diagram of the robot arm pressing the brush to the surface of the duct. Figure 4 illustrates the forces acting on the surface and brushes. In this model, only the normal forces to the surface are considered and tangential force including the friction force of the surface is neglected. Spring constant of the compliant device is considered as relatively very small compared to the elasticity of the brush, which can also ignore the extra effect for measuring force caused by the device.

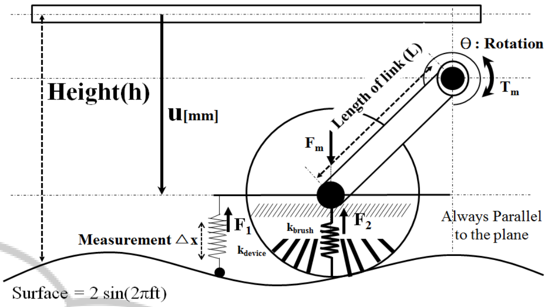

Figure 3: Free Body Diagram of the rotating brush of the robot arm contacting the surface of the duct.

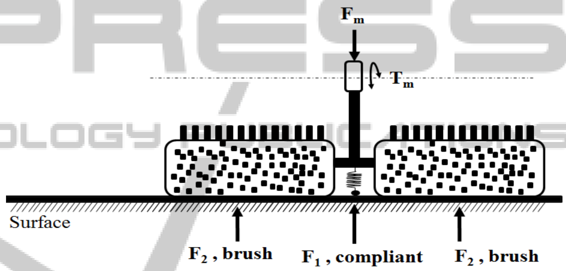

Figure 4: Frontal View of force equilibrium of pushing the brush and elastic forces of compliant device and brush.

The force acting on the robot arm(F_m) can be expressed by

$$F_m = \frac{T_m \times N}{L sin\theta} \tag{1}$$

where T_m : the motor torque,
N : gear reduction ratio,
L : effective length of the link.

From Figure 4 the motor torque can be calculated from the force equilibrium equation given by

$$F_m = F_1 + 2F_2 \tag{2}$$

$$\mathrm{T_m} = \frac{\mathrm{Lsin\theta}}{\mathrm{N}} (\mathrm{F_1} + 2\mathrm{F_2}) \tag{3}$$

where $F_1 = k \times \Delta x$, $F_2 = ax^2 + bx$ .the Δx is a spring deformation, k is a spring constant of the compliant device, and F_2 is assumed as the 2[nd] order displacement of spring by pressing.

Since the actual characteristic of the stiffness of the brushes shows nonlinear behaviour against external force, the stiffness of the rotating brush has been modelled as 2[nd] order polynomial function. Therefore, simple nonlinearly elastic characteristic is used to reveal feasibility of the force control with the spring deformation feedback. Figure 5 shows the prototype of the robot arm brush with a compliant device to measure the deformation of the spring.

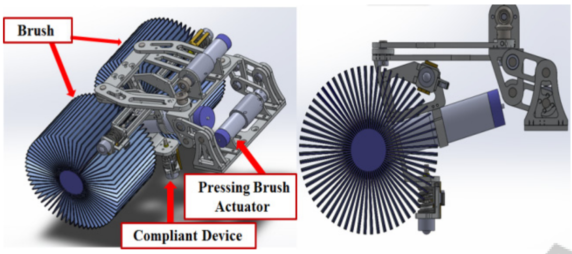

Figure 5: Modelling of Robot arm brush with compliant device.

2.2 Motor Dynamics and Control

The simple DC motor dynamic model shown in Figure 6 is used in simulation with MATLAB® SIMULINK® tool. The model is consisted of linear differential equations of mechanical and electrical system summarized at Eq.(4) and Eq.(5). Each motor parameter and values are summarized in Table 1.

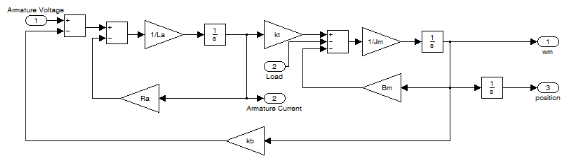

Figure 6: Motor Dynamic Model implemented by MATLAB® SIMULINK®.

Table 1: DC Motor Specification.

Parameter		Value
J_m	Rotor inertia	10.8 gcm^2
B	Speed/Torque gradient	40.3 rpm/mNm
K_t	Torque Constant	23.4 mNm/A
K_b	Speed Constant	408 rpm/V
L_a	Terminal Inductance	0.238 mH
R_a	Terminal Resistance	2.32 Ω

$$i_a(t) = \frac{1}{L_a}\int_0^t [V_a(\tau) - R_a i_a(\tau) - e_a(\tau)]d\tau \tag{4}$$

$$\mathrm{w_m}(t) = \frac{1}{J_m}\int_0^t [T_e(\tau) - Bw_m(\tau) - T_L(\tau)]d\tau \tag{5}$$

$$e_a = K_b w_m(t) \tag{6}$$

$$T_m = K_t i_a(t) \tag{7}$$

where T_L Load from the end of the motor axis, T_e is torque proportional to the current i_a, and e_a is back electro-motive force from the coil of the motor

The rotation angle of the motor $\theta_m(t) = \theta_2(t)$ is obtained from angular velocity of $w_m(t)$. The load value for the DC motor is also induced from the weight of the robot arm brush. Therefore, the torque generated by the motor Eq.(3) can be calculated as following

$$T_m = \frac{Lsin\theta}{N}(F_1 + 2F_2 - Mg) \tag{8}$$

where T_m : the motor torque,
N : gear reduction ratio,
L : effective length of the link,
M: mass of the robot arm linkage.

2.3 Force Control

Based on the Hooks Law of the spring-based compliant device, the force of the compliance can be calculated from the deformation generated by the brush(robot arm) moving vertically. The relationship between the position of the brush and deformation of the spring can be expressed as follows

$$\Delta \mathrm{x} = \mathrm{l_0} - l = l_0 - \mathrm{Height} + \mathrm{u} \tag{9}$$

$$Height = 0.148 + 0.002\sin(2\pi \mathrm{ft}) \tag{10}$$

where l_0 is the initial length of the spring and u is vertical position of the brush.

The *Height* variable was defined as the length from the top of the duct. The irregularity of duct surface was modelled with sinusoidal function and sensing disturbance was also added to the control model shown in Figure 7. Finally, the Figure 7 illustrates the dynamic model of the force control of the brush with the compliant device.

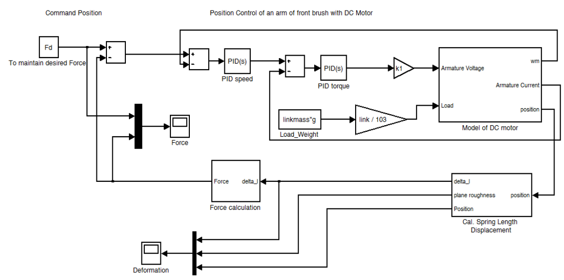

Figure 7: Force control model with deformation feedback.

The force control model has been simulated with PID control gains as summarized in Table 2. Figure 8 shows the schematic diagram of the robot control system including host computer and communication.

Table 2: PID Gains for Force Control of Robot Arm.

Gain		Value
Speed control	P	2.114
	I	8.853
	D	-0.002
Torque control	P	0.166
	I	11.807
	D	0

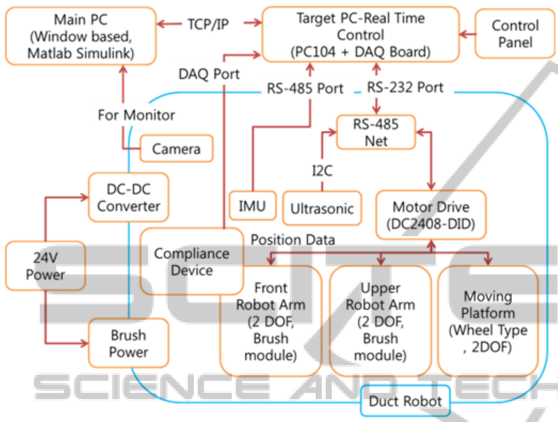

Figure 8: Schematic diagram of the robot control system and communication.

3 SIMULATION RESULTS

The spring constant (k) of the compliant device used in the simulation is 0.3[N/m], and coefficients for the nonlinear brush stiffness is assumed as values of a=2000[N/m^2], and b=4500[N/m], which is expressed in the Eq.(2). It is also considered that the maximum allowable displacement of the spring to the geometry including the diameter of the brush is 100mm and the height of the duct is 150mm. The k is exerted by that of value installed to the prototype robot. However, constants of the nonlinear stiffness brush are decided arbitrary which is relatively higher than that of compliant spring. At first, the simulation results are shown in Figure 9 controlling the force from deformation feedback to satisfy the desired force by moving the brush on the sinusoidal surface.

Figure 9(a) shows the result of force control that of maximum error is 1% to the objective force and the spring is deformed below the limit (0.05m) of the geometric interference.

Next, the sinusoidal surface function is changed by adding disturbances signal whose maximum level is 1/25 of the magnitude of sinusoidal function. Results are presented in Figure 10. The error bound is $\pm$1N similar to that of previous results shown in Figure 8(a). The Pressing force of the brush has been controlled with the spring-based force compliant device whose results are depicted in Figure 9, and 10. In addition, the nonlinear behaviour of the brush stiffness has not been considered, that is, the brush stiffness has been modelled as a linear spring.

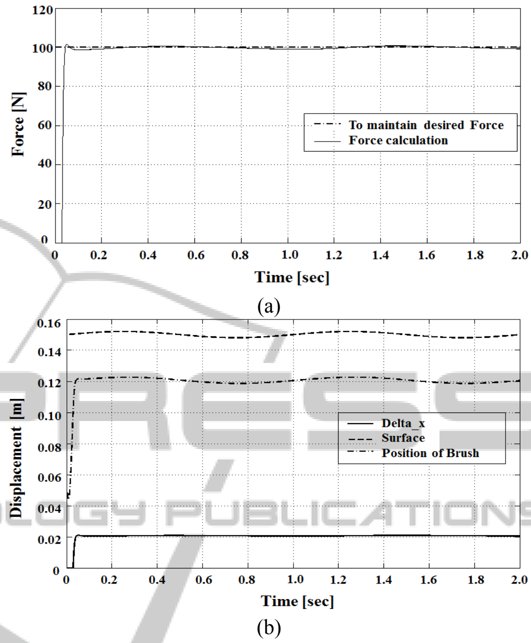

Figure 9: Results of Force Control at 2mm, 1Hz sinusoidal function of Surface. (a) Measured Force, (b) Displacement.

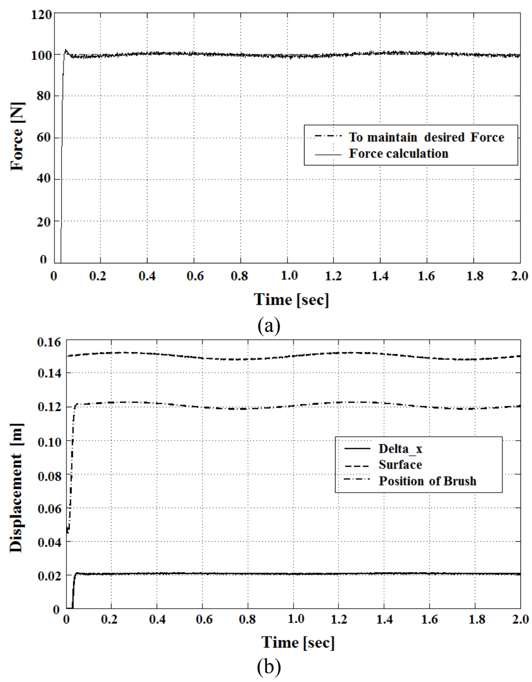

Figure 10: Results of Force Control at 2mm, 1Hz sinusoidal function with 1/25 disturbances of Surface. (a) Measured Force, (b) Displacement.

4 CONCLUSIONS

In this study, the cleaning force control of the rotating brush has been conducted by utilizing the spring-based simple compliant device. It is also assumed that the stiffness of the brush is modelled as nonlinear function with 2nd order polynomials about displacement to reflect nonlinear characteristics of the brush. In results, the cleaning force can be successfully controlled with the simple compliant device. In future study, some simplifications and assumptions such as tangential force on the surface can be partially considered for more accurate results. Furthermore, it is also necessary to consider dynamic model of rotating brush. The simulation results will be further verified under the test-bed environment using the prototypes of the duct cleaning robot.

ACKNOWLEDGEMENTS

This research has been conducted as a part of the subway air duct cleaning robot project (Eco-Innovation, No. E211-40002-0003-0) partially funded by the Ministry of Environment in Korea.

REFERENCES

Brosseau, L. M., Vesley, D., Kuehn, T. H., Melson, J., Han, H.S. 2000. 'Duct cleaning: A review of associated health effects and results of company and expert surveys', *ASHRAE Trans*, 106, 180-187.

Finnish Society of Indoor Air Quality and Climate (FiSIAQ). 2001. Classification of indoor climate 2000, Espoo, Finland.

Jeong, W., Jeon, S. W., Park, D., Kwon, S. B., 2012. 'Force Control of a Duct Cleaning Robot Brush Using a Compliant Device, *10th International Conference on Informatics in Control, Automation and Robotics(ICINCO) 2012*, Roma, Italy.

Robotics Design, ANATROLLER ARI-100, http:// www.roboticsdesign.qc.ca/mobile-robots, Canada.

Wang, Y., Zhang, J., 2006. 'Autonomous Air Duct Cleaning Robot System,' *Proc. of International Midwest Symposium on Circuits And System*, pp. 510-513, 2006.

Motor Specification, RE Ø25mm, Graphite Brushes, 20W, http://www.maxonmotor.com/maxon/view/product/motor/dcmotor/re/re25/118752, Switzerland.

Kim, S.H. 2007. 'Control of DC and AC Motor'. *Buk-du Press*, Seoul: 96-103.